Coherent Communications for Free Space Optical Low-Earth Orbit Downlinks

Balázs Matuz[†], Ayman Zahr[†], Alexander Sauter[†]
[†]Institute of Communications and Navigation, German Aerospace Center (DLR), Germany

***Abstract*—This work addresses physical layer design aspects of coherent free-space optical downlinks from low-earth orbit satellites to ground. Achievable information rates are derived and assessed that include the availability of diversity, shaping, bit-metric decoding, repetition coding and automatic repeat request with maximum-ratio combining. A channel coding scheme is presented that approaches the theoretic limits within 1 dB. Extrinsic information transfer analysis for the free-space optical fading channel shows that a code design tailored to the additive white Gaussian noise channel is robust for fading channels with various parameters.**

I. Introduction

Free-space optical (FSO) satellite links complement radio frequency (RF) links and may serve the increasing demand for bandwidth. While current RF systems can sustain data rates of at most some Gbps, FSO links target data rates of tens to hundreds of Gbps [1]. Such high data rates are particularly interesting for low earth orbit (LEO) satellite downlinks: the LEO satellite is only visible for a few minutes (between 5 and 15) in which the data transfer from the satellite to ground takes place. A key enabler for high data rates are higher order (coherent) modulation techniques paired with powerful forward error correction (FEC) schemes which are widely used in fiber optical systems [2] but are non-standard for FSO links.

Due to the high frequency of the optical signal, the FSO communication channel is prone to undesired impairments [3].[1] One effect is scintillation (the analog of fading in RF systems) which refers to fluctuations of the signal amplitude due to the changing characteristics of the transmission medium (air). It is well-established that with channel state information (CSI) at the receiver (RX) the ergodic capacity of fading channels is at most the capacity of an additive white Gaussian noise (AWGN) with the same signal-to-noise ratio (SNR) [4]. For non-ergodic fading channels the Shannon capacity is often zero. In this case, additional countermeasures in terms of diversity techniques are employed.

This work considers coherent transmission over FSO LEO downlinks. We derive achievable information rates to provide insight into the system design and to provide a suitable channel code design. Different assumptions on the communication system are investigated, for instance the impact of diversity, the type of information the decoder is able to process, a shaping code, maximum-ratio combining (MRC) and automatic repeat request (ARQ) techniques. Finally, low-density parity-check (LDPC) codes are shown to approach the computed rates closely. A protograph extrinsic information transfer (EXIT) analysis [5] for the FSO fading channel suggests that code ensemble designed for the AWGN channel are a robust choice for FSO downlinks.

[1]In fact, also modern RF satellite systems exploit higher frequency bands for transmission, such as the Q/V bands and hence are subject to undesired channel impairments.

978-1-6654-3540-6/22 © 2022 IEEE

II. Preliminaries

A. Protograph LDPC codes

Let $\mathcal{C}(n,k)$ be a binary channel code with block length n and information length k. The code rate is $\mathsf{R_c} = k/n$. The code is described by an $m \times n$ parity-check matrix $\boldsymbol{H}$ where we assume $m = n - k$. Let the modulation order be M, the transmission rate $\mathsf{R} = \mathsf{R_c} b$, where $b = \log_2 M$ is the number of bits per modulation symbol. We will consider structured, protograph LDPC codes [6]. A protograph is a small bipartite graph that can be described by an $m_b \times n_b$ adjacency matrix or base matrix $\boldsymbol{B} = [b_{i,j}]$. The bipartite graph of an LDPC code is obtained by copying the protograph Q times and interconnecting the edges of the copies. This is called lifting or expansion and is detailed in [6]. We obtain $n = n_b Q$, $m = m_b Q$.

B. EXIT analysis

A common tool to predict the asymptotic performance (for large n) of an LDPC code ensemble is density evolution [7] or its approximation EXIT analysis [8]. The latter estimates the ensemble's iterative decoding threshold $(\frac{E_s}{N_0})^\star$ which is the smallest value of $\frac{E_s}{N_0}$ such that the symbol error probability vanishes as the number of decoding iterations and the block length go towards infinity. In this work, we use protograph EXIT analysis [5] and an optimization tool to identify code ensembles with good iterative decoding thresholds.

C. Channel model

To model transmission from a LEO satellite to ground, we consider the following simplified discrete-time channel model [3], [9], [10]

$$y_i = \sqrt{h_i} x_i + n_i. \tag{1}$$

In (1) y_i is the received symbol (after matched filtering and synchronization), h_i the channel power gain, x_i the transmitted modulation symbol, and n_i the AWGN. For ease of presentation, we consider one dimension of the signal for analysis, i.e., the in-phase (or alternatively quadrature) component. The

modulation symbol x_i is thus an M-ary amplitude shift keying (ASK) symbol (rather than a complex quadrature amplitude modulation (QAM) symbol).

We denote random variables (r.v.s) by uppercase letters and their realisations by lowercase letters. We assume that the r.v. H_i is real and log-normally (LN) distributed, i.e., $H_i \sim \mathcal{LN}(m_h, s_h^2)$. The complex phase is assumed to be compensated by appropriate synchronisation algorithms [11]. Without loss of generality we impose

$$\mathrm{E}\left[H_i\right] = \exp\left(m_h + \frac{s_h^2}{2}\right) \stackrel{!}{=} 1$$

i.e., $m_h = -\frac{s_h^2}{2}$. Let the noise be Gaussian distributed, i.e., $N_i \sim \mathcal{N}(\mu_n, \sigma_n^2)$ and define the energy per symbol to noise power spectral density ratio as

$$\frac{E_s}{N_0} = \frac{1}{\sigma_n^2}. \tag{2}$$

We will refer to the quantity in (2) as SNR. We distinguish between the following channel models:

- Fast (or ergodic) fading channel: H_i are independent and identically distributed (i.i.d.) r.v.s for all $i \in \{1, \ldots, n/b\}$ modulated codeword symbols. This is a reasonable assumption, e.g., when long physical layer interleavers can be applied.
- Block fading channel: the modulated codeword is partitioned into L blocks. H_i is constant per block, while for different blocks the power gains are i.i.d. r.v.s. This simplified model is commonly used for information theoretic analysis.
- Correlated fading channel: H_i are dependent and identically distributed. The auto-correlation function or alternatively the power spectral density (PSD) of the random process is taken from the literature [12].

III. Rate computation

A. Ergodic capacity

The capacity C is the maximum mutual information (MI) between the channel input X and channel output Y, i.e.,

$$\mathsf{C} = \max_{P(x)} \mathsf{I}(X;Y)$$

The capacity C_{LN} of the log-normal (LN) fast fading channel is

$$\mathsf{C}_{\mathsf{LN}} = \max_{P(x)} \int_0^\infty \mathsf{I}\left(X;Y|H=h\right) p(h)\,\mathrm{d}h. \tag{3}$$

The MI $\mathsf{I}\left(X;Y|H=h\right)$ in (3) corresponds to the MI of an AWGN channel with SNR $\gamma = h\frac{E_s}{N_0}$ where γ is also referred to as instantaneous SNR.

B. Outage capacity of block fading channel

When the codeword duration is in the order of the channel coherence time, the Shannon capacity of the LN fading channel is zero. This is since very low channel gains occur with non-zero probability (the so-called outage probability) and error-free decoding is only possible when the rate tends to zero. We consider the block fading channel with L blocks per codeword and define the outage probability as

$$p_{\mathsf{out}}(\mathsf{R}) = \Pr\left\{\max_{P(x)} \frac{1}{L}\sum_{\ell=1}^{L} I(X,Y,H_\ell) < \mathsf{R}\right\} \tag{4}$$

where the r.v. $I(X,Y,H_\ell)$ denotes the rate supported by the channel in block ℓ and it takes values $\mathsf{I}(X;Y|H_\ell = h)$.

Example 1. In case of the unconstrained input AWGN channel (with block fading) we obtain

$$I(X,Y,H_\ell) = \frac{1}{2}\log_2\left(1 + H_\ell\frac{E_s}{N_0}\right).$$

The distribution of $I(X,Y,H_\ell)$ is obtained from the distribution of H_ℓ by transformation of r.v.s.

The $\epsilon-$outage capacity is the maximum transmission rate such that the outage probability is smaller than a fixed value ϵ, i.e.,

$$\mathsf{C}_\epsilon = \operatorname*{argmax}_{\mathsf{R}} p_{\mathsf{out}}(\mathsf{R}) < \epsilon. \tag{5}$$

(5) can be computed numerically by the Monte Carlo method and implies that we can communicate error-free (at least) a fraction of time which is $1-\epsilon$. Then, in average we can communicate error free with a rate

$$\bar{\mathsf{R}}_\epsilon = (1-\epsilon)\mathsf{C}_\epsilon.$$

Average rates $\bar{\mathsf{R}}_\epsilon$ versus $\frac{E_s}{N_0}$ for uniform and shaped 4-ASK are depicted in Fig. 1 for the AWGN channel, the fast fading channel, and the block fading channel with $\epsilon = 10^{-2}$. 4-ASK (or 16-QAM) modulation is of high interest for upcoming FSO satellite systems and thus will be considered as a baseline for the results. Literature [13] provides representative values of the power scintillation index S which can be converted to s_h^2 as

$$s_h^2 = \ln(1+S).$$

For the plots we selected $s_h^2 = 0.1$ which is typical for weak turbulence, an elevation of 10°, a wavelength of 847 nm, and an aperture size of 40 cm. A broader set of values for s_h^2 and ϵ is considered in Tables I and II, respectively. Observe from Fig. 1 that the maximum shaping gain for the LN fading channel is around 0.39 dB while it is around 0.44 dB on the AWGN channel (not shown).[2] Table I shows that the shaping gain decreases with increasing s_h^2. Likewise, for $s_h^2 = 0.1$ and $\epsilon = 10^{-2}$ the figure shows a gap of 0.188 dB between the ergodic LN fading channel and the AWGN channel capacity, at rate $\mathsf{R} = 1$. In case of the block fading channel with one block ($L = 1$) we observe a gap of 3.3 dB with respect to the ergodic channel. Diversity considerably helps to reduce the gap, e.g., to 1.23 dB for $L = 8$. In case of stricter requirements on ϵ the gap to the ergodic rate increases up to 2.11 dB for $\epsilon = 10^{-5}$ and $L = 8$, as shown in Table II. In fact, we observe

[2]For 8-ASK (64-QAM) the shaping gain is around 0.8 dB for an AWGN channel. Due to practical reasons we restrict to lower modulation orders.

TABLE I
MAXIMUM SHAPING GAIN ON THE FAST LN FADING CHANNEL FOR DIFFERENT VALUES s_h^2.

s_h^2	0.01	0.05	0.1	0.2	0.3	0.4
Gain [dB]	0.43	0.41	0.39	0.36	0.33	0.31

TABLE II
GAP BETWEEN FAST AND BLOCK FADING CHANNEL AT RATE $\mathsf{R} = 1$ FOR VARIOUS ϵ AND L.

	$L = 1$	$L = 4$	$L = 8$	$L = 16$
$\epsilon = 10^{-2}$	3.30 dB	1.69 dB	1.23 dB	0.88 dB
$\epsilon = 10^{-4}$	5.14 dB	2.55 dB	1.82 dB	1.29 dB
$\epsilon = 10^{-5}$	5.93 dB	3.03 dB	2.11 dB	1.57 dB

that the gap to the ergodic LN fading channel increases with decreasing ϵ and decreases with the number of blocks per codeword L.

Remark 1. The simplified block fading channel model gives insights on the dimensioning of the channel interleaver. For instance, the length of a block can be considered as a proxy of the channel's coherence time. Then, Fig. 1 gives a prediction on the achievable rates for an interleaver spanning over L times the coherence time. The accuracy of this assumption is illustrated in Fig. 5.

C. Achievable rates for bit metric decoders

When using higher-order modulations with binary codes we experience a potential rate loss. Let the bit label of the modulation symbol X be $\boldsymbol{B} = [B_1, \ldots, B_b]$. For decoders using a bit metric an achievable rate is [14]

$$I_{\mathsf{BMD}}(X,Y,H) = \left[\sum_{i=1}^{b} I(B_i,Y,H) - \sum_{i=1}^{b} \mathsf{H}(B_i) + \mathsf{H}(\boldsymbol{B})\right]^+ \leq I(X,Y,H). \tag{6}$$

The r.v. $I(B_i,Y,H)$ denotes the rate of bit channel B_i. It takes values $\mathsf{I}(B_i;Y|H=h)$ which can be easily computed [15].

To compute the outage capacity under bit metric decoding we use (6) in (5). Fig. 1 exemplifies the minimal rate loss under bit metric decoding (BMD) on the LN fading channel. In general, we found that rate loss under BMD is marginal for the LN fading channel considered in this work. The statement holds both when $P(x)$ is optimized (shaping), as well as when $P(x) = 1/M$ for all x (uniform).

D. Repetition with maximum-ratio combining

Repetition is a potential technique for FSO links in order to provide additional diversity [16]. Let us consider a block fading channel for which the channel gain is constant over a codeword (with $L = 1$). Let us assume that at the receiver we observe T different copies of a codeword symbol, each of

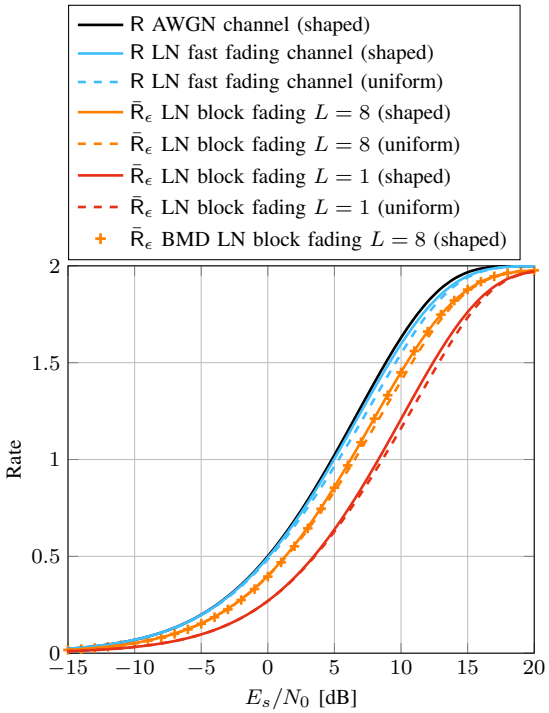

Fig. 1. Rates LN (block) fading channel with $s_h^2 = 0.1$, 4-ASK, $\epsilon = 0.01$.

which experiences i.i.d. channel gains. With MRC at the RX, the instantaneous SNR at the combiner output is

$$\Gamma_{MRC} = \frac{E_s}{N_0} \underbrace{\sum_{t=1}^{T} H_t}_{H_{MRC}}. \tag{7}$$

The outage probability for the r.v. $I(X,Y,H_{MRC})$ is obtained from (4), where H_{MRC} is defined in (7). The outage capacity is then obtained from (5). Assume that the copies of a codeword symbol are obtained by T channel uses. The average rate at which we can communicate error free is

$$\bar{\mathsf{R}}_\epsilon = \frac{1}{T}(1-\epsilon)\mathsf{C}_\epsilon.$$

Rates $\bar{\mathsf{R}}_\epsilon$ for MRC versus $\frac{E_s}{N_0}$ for uniform 4-ASK with $\epsilon = 10^{-2}$ are depicted in Fig. 2. As a reference, rates for the uniform fast fading channel and the uniform LN block fading channel are shown as well. Observe that repetition of the codewords (and MRC at the RX) shows big losses with respect to the competitors. In fact, it may yield worse performance than a scheme with comparable overall rate, but no diversity at all ($L = 1$). Only when transmission rates get very low, repetition with MRC is a viable option.

E. Automatic repeat request

ARQ is considered in FSO systems as an alternative to long physical layer interleaving to increase diversity [17]. Let $P(X = t)$ be the probability of successful decoding after the tth round of transmission with $1 \leq t \leq T$, T being

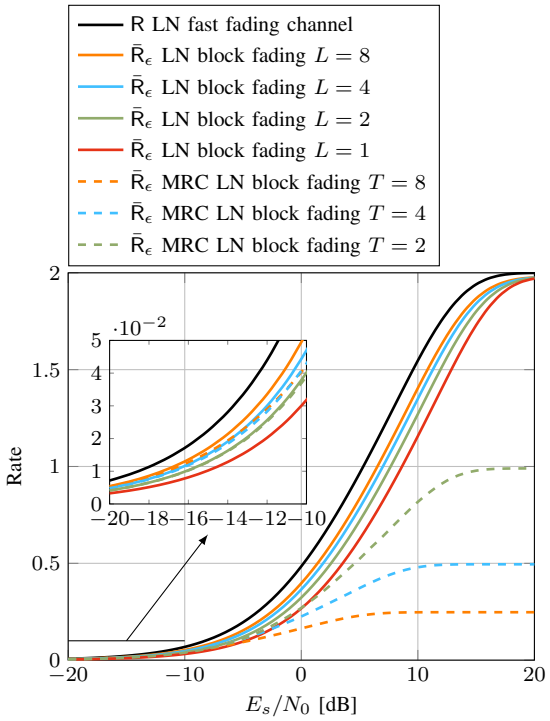

Fig. 2. Rates uniform LN (block) fading channel with repetition and MRC with $s_h^2 = 0.1$, 4-ASK, $\epsilon = 0.01$.

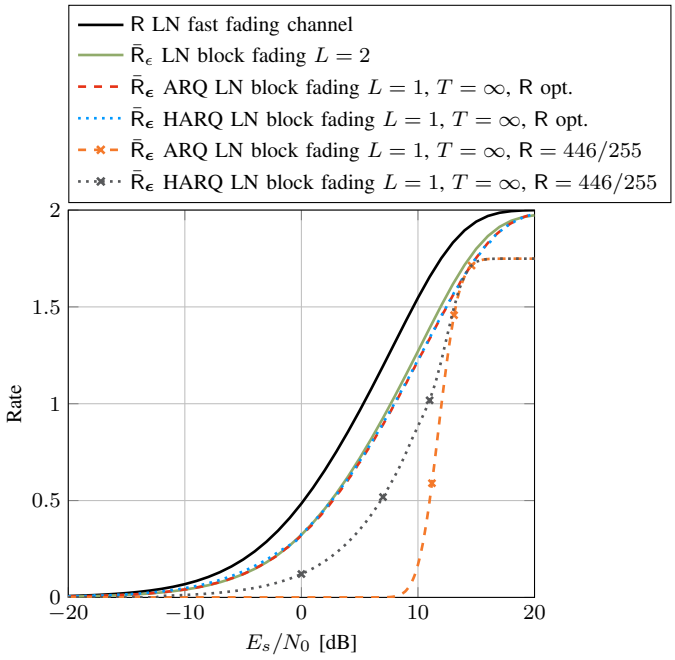

Fig. 3. Rates uniform LN (block) fading channel and ARQ/HARQ with MRC assuming $s_h^2 = 0.1$, 4-ASK, $\epsilon = 0.01$.

the maximum number of transmissions. With slight abuse of notation let ϵ_i be the outage probability at the ith round, where

$$P(X = t) = \prod_{i=1}^{t-1} \epsilon_i (1 - \epsilon_t).$$

With $\boldsymbol{\epsilon} = [\epsilon_1, \epsilon_2, ..., \epsilon_T]$ the average rate is

$$\bar{\mathsf{R}}_{\boldsymbol{\epsilon}} = \frac{\mathsf{R}}{\mathrm{E}[X]} \tag{8}$$

For the special case of $\epsilon_i = \epsilon$ and $T = \infty$, we obtain

$$\mathrm{E}[X] = \frac{1}{1 - \epsilon}.$$

The expression in (8) is maximized by properly choosing the outage probability ϵ, or equivalently the transmission rate R which is related to the outage probability by (4) ($L = 1$). Likewise, we consider hybrid automatic repeat request (HARQ) with MRC, also referred to as Chase combining. The instantaneous SNR at the combiner output at the ith transmission round is given by (7) and ϵ_i can be computed as a function of R from (4).

Fig. 3 shows average rates $\bar{\mathsf{R}}_{\boldsymbol{\epsilon}}$ for ARQ and HARQ with MRC for $T = \infty$ assuming that the transmission rate is optimized for each $\frac{E_s}{N_0}$. It turns out that $\mathrm{E}[X]$ is close to one particularly for moderate/high $\frac{E_s}{N_0}$ (not shown), i.e., re-transmissions occur rarely. Overall, the average rate curve for (H)ARQ is close to the one for the block fading channel with $L = 2$ which implies a notable loss compared to the fast fading channel. Also, one may assume a fixed transmission rate due to practical limitations. In this case, we observe a loss compared to the optimized (H)ARQ curves, except for a specific operating point. For instance, in case of $\mathsf{R} = 2 \cdot 223/255$ the operating point is around $\frac{E_s}{N_0} = 14.5$ dB and $\bar{\mathsf{R}}_{\boldsymbol{\epsilon}} = 1.7$. At an average rate of $\bar{\mathsf{R}}_{\boldsymbol{\epsilon}} = 0.5$ the difference in terms of $\frac{E_s}{N_0}$ for ARQ compared to the LN fast fading channel is around 11 dB, whereas for HARQ with MRC it is around 7 dB. In Fig. 3 the three 'x'-markers subdivide the (H)ARQ curves into four different segments. Points (rates) on the rightmost segment are achievable for $T \geq 2$, on the middle-right for $T \geq 4$, on the middle-left for $T \geq 16$, and on the leftmost segment for $T = \infty$.

IV. LDPC CODE DESIGN

For LEO downlinks with data rates of tens of Gbps LDPC codes are excellent candidates since the decoder is placed on ground and severe constraints only apply to the encoder on board of the satellite. Currently, LDPC codes are subject to Consultative Committee for Space Data Systems (CCSDS) standardization for FSO downlinks with on-off keying (OOK) [18]. Next, we present a methodology for the LDPC code design for coherent communications, paired with a code design example. In particular, the code design is performed on a surrogate binary-input AWGN channel with adaptations to support higher order modulations and fading. This is since LDPC codes are known to be *universal*, i.e., code designs for one channel usually perform well also on other channels.

A. Binary input AWGN channel code design

For ease of presentation, we consider an accumulate-repeat-accumulate (ARA) protograph LDPC code design with linear

encoding complexity in n [19]. Particularly for small protographs the exploration space is limited due to the fixed ARA structure [19]. A search for protographs with good iterative decoding thresholds can be done via suitable optimization algorithms, such as differential evolution.

Example 2. Consider a target code rate of $\mathsf{R}_\mathsf{c} = 1/2$. Fixing the base matrix size to $n_b = 5$ and $m_b = 3$ we obtain

$$\boldsymbol{B}_1 = \begin{bmatrix} \textcircled{3} & \textcircled{1} & 0 & 1 & 1 \\ 1 & \textcircled{3} & 0 & 1 & 1 \\ 2 & 0 & 1 & 0 & 0 \end{bmatrix}.$$

All variable nodes (VNs) associated to the first column of $\boldsymbol{B}_1$ are punctured. The entries subject to optimization are encircled. The iterative decoding threshold on the binary-input additive white Gaussian noise (biAWGN) channel is $(\frac{E_s}{N_0})^\star = 0.58$ dB.

B. Modifications of protograph EXIT analysis

1) EXIT analysis for higher order modulations: We assume BMD where each of the b bit channels is modeled by a biAWGN channel. More specifically, we evaluate the conditional entropy $\mathsf{H}(B_i|Y)$ of each bit channel and match it with the conditional entropy $\mathsf{H}(X|Y)$ of a surrogate biAWGN channel. This way, standard protograph EXIT analysis can be applied to obtain an estimate of the code ensemble's iterative decoding threshold [20]. The mapping of the $n_b - 1$ (not punctured) VN types in the protograph to the b bit channels impacts the threshold. We perform an optimization of this mapping. It turns out that a random assignment of the bit channels to the n code bits yields only minor losses (Fig. 4).

2) EXIT analysis for fast fading channels: Each of the Q VNs of the code associated to a specific VN type receive channel messages from fading channels with i.i.d. power gains. Thus for a (not punctured) VN type in the protograph we compute an average MI at its output, where averaging is done over the different parameters of the channel message. Formally, let $\mathsf{I}_{Ev|\ell}$ be the MI between the ℓth VN output message and the associated codeword bit, I_{ch} the MI between the channel observation and the associated codeword bit, and $\mathsf{I}_{Av|\ell}$ be the MI between the ℓth VN input message and the associated codeword bit [5]. We modify the computation of the extrinsic information at the VNs as

$$\mathsf{I}_{Ev|\ell} = \mathrm{E}\left[f(\mathsf{I}_{Av|1}, ..., \mathsf{I}_{Av|\ell-1}, \mathsf{I}_{Av|\ell+1}, ..., \mathsf{I}_{Av|d_v}, I_{ch})\right]$$

where $f(\cdot)$ is the VN EXIT function, d_v is the VN degree, and the expectation is done over the r.v. I_{ch}.

3) EXIT analysis for block fading channels: Consider a block fading channel with L blocks. By EXIT analysis we can determine the L-dimensional convergence region (outage limit) of a protograph LDPC code ensemble which are all admissible values of $\Gamma_\ell = H_\ell \frac{E_s}{N_0}$, $\ell \in \{1, \ldots, L\}$ such that EXIT analysis converges [21]. We are interested in a related quantity, namely the outage probability of the ensemble which is obtained through Monte Carlo simulations: for a specific $\frac{E_s}{N_0}$ we draw L i.i.d. samples of the power gain and compute the conditional entropy of the $b \cdot L$ bit channels and proceed as in IV-B1. EXIT analysis will either declare convergence or decoding failure. We repeat the experiment m_c times and count the number of decoding failures e. Then, e/m_c gives an estimate on the outage probability p_{out} of a specific protograph LDPC code ensemble. The mapping between VN types and blocks of the block fading channel is optimized, but a random permutation of the code bits turns out to be a good choice.

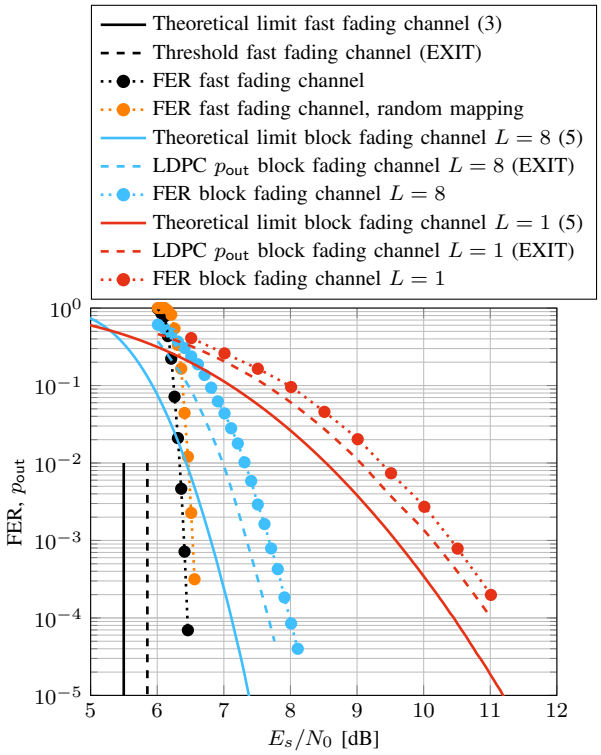

Fig. 4. Theoretical limits, thresholds, and FER versus $\frac{E_s}{N_0}$ for $(30720, 15360)$ LDPC code from $\boldsymbol{B}_1$ over LN (block) fading channel and uniform 4-ASK.

C. Simulation results

1) Frame error rates for fast and block fading channels: The frame error rate (FER) over the fast fading channel and the outage probability over the block fading channel with $L \in \{1, 8\}$ of a $(30720, 15360)$ ARA LDPC code with base matrix $\boldsymbol{B}_1$ is depicted in Fig. 4. In addition, we plot the theoretic limit/outage probability for a capacity achieving code using (3) and (5), as well as the LDPC code ensemble's iterative decoding threshold/outage probability. Observe that we experience a loss between the theoretical limits and the asymptotic performance of the ensemble due to the suboptimality of the code design and an additional loss due to finite length effects. However, the proposed LDPC code performs within 1 dB from the theoretic limits over the different LN fading channels which confirms the validity of the code design.

2) Frame error rate for correlated fading channel: We consider a correlated LN fading channel (see Section II-C) and empirically define the coherence period as the number of symbols after which the auto-correlation function drops

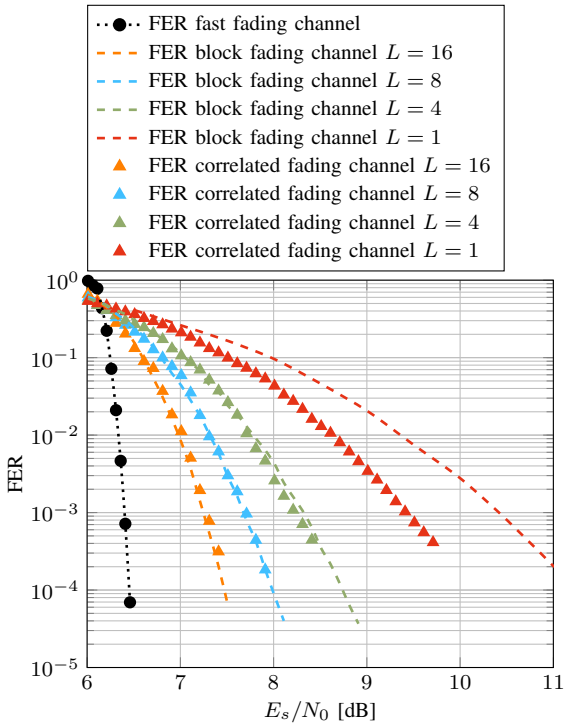

Fig. 5. FER versus $\frac{E_s}{N_0}$ for $(30720, 15360)$ LDPC code from $\boldsymbol{B}_1$ with 4-ASK over LN block fading channel with $L \in \{1, 4, 8, 16\}$, as well as correlated fading channel with interleaving over $L \in \{1, 4, 8, 16\}$ coherence periods.

by 8 dB. Let the channel interleaver span over L coherence periods. The FER of the proposed ARA LDPC code versus $\frac{E_s}{N_0}$ is depicted in Fig. 5. For comparison, the FER over a block fading channel with L blocks is also shown. Observe that the block fading channel is too pessimistic for $L = 1$ due to the constant channel gain over an entire block (codeword). By contrast, for $L \geq 4$ the block fading channel turns out to be a reasonably good proxy of the correlated fading channel.

Remark 2. While rates for the block fading channel can be easily obtained (see Section III), the analysis of a general correlated channel is more cumbersome.

V. Conclusion

This work derives information rates for the coherent FSO LEO downlinks. We find that the shaping gain for 4-ASK (16-QAM) is limited to around 0.3 dB so that additional implementation complexity of a shaping code might not justify its use for such low modulation orders. We find that BMD on the fading channel performs similarly to coded modulation, i.e, there is virtually no penalty in using binary codes. Repetition coding with MRC for increased diversity turns out to be an unfavorable choice, even compared to a coded scheme without any diversity (at least for transmission rates above 0.4 bits per channel use). Similar conclusions hold for ARQ and HARQ with MRC. Furthermore, we propose practical LDPC codes whose encoders can be implemented on-board of a satellite and which perform within 1 dB from theoretical limits. Based on techniques from the literature, we modify EXIT analysis and determine iterative decoding thresholds, as well as outage probabilities for protograph LDPC code ensembles over the FSO fading channel. Asymptotic results show that an AWGN code design is robust for various fading channel parameters, where the loss to theoretic limits is between 0.3 dB and 0.6 dB.

References

[1] M. A. Khalighi and M. Uysal, "Survey on free space optical communication: A communication theory perspective," *IEEE Commun. Surveys Tuts.*, vol. 16, no. 4, pp. 2231–2258, 2014.

[2] *Interfaces for the optical transport network*, ITU-T G-Series Recommendations, International Telecommunication Union (ITU) Recommendation ITU-T G.709/Y.1331, Jun. 2020.

[3] X. Zhu and J. M. Kahn, "Free-space optical communication through atmospheric turbulence channels," *IEEE Trans. Commun.*, vol. 50, no. 8, pp. 1293–1300, 2002.

[4] D. Tse and P. Viswanath, *Fundamentals of wireless communication*. Cambridge university press, 2005.

[5] G. Liva and M. Chiani, "Protograph LDPC codes design based on EXIT analysis," in *Proc. IEEE Global Telecommun. Conf.*, Nov. 2007, pp. 3250–3254.

[6] J. Thorpe, "Low-density parity-check (LDPC) codes constructed from protographs," NASA JPL, Pasadena, CA, USA, IPN Progress Report 42-154, Aug. 2003.

[7] T. J. Richardson and R. L. Urbanke, "The Capacity of Low-Density Parity-Check Codes under Message-Passing Decoding," *IEEE Trans. Inf. Theory*, vol. 47, no. 2, pp. 599–618, 2001.

[8] A. Ashikhmin, G. Kramer, and S. ten Brink, "Extrinsic information transfer functions: Model and erasure channel properties," *IEEE Trans. Inf. Theory*, vol. 50, no. 11, pp. 2657–2673, 2004.

[9] A. Al-Habash, L. C. Andrews, and R. L. Phillips, "Mathematical model for the irradiance probability density function of a laser beam propagating through turbulent media," *Optical engineering*, vol. 40, no. 8, pp. 1554–1562, 2001.

[10] A. Belmonte and J. M. Kahn, "Performance of synchronous optical receivers using atmospheric compensation techniques," *Optics express*, vol. 16, no. 18, pp. 14 151–14 162, 2008.

[11] M. Niu, J. Cheng, and J. F. Holzman, "Error rate analysis of m-ary coherent free-space optical communication systems with k-distributed turbulence," *IEEE Trans. Commun.*, vol. 59, no. 3, pp. 664–668, 2011.

[12] D. Giggenbach, A. Shrestha, F. Moll, C. Fuchs, and K. Saucke, "Reference power vectors for the optical leo downlink channel," in *Int. Conf. Space Opt. Sys. and Appl. (ICSOS)*, Portland, OR, USA, Oct. 2019, pp. 1–4.

[13] M. Brechtelsbauer, D. Giggenbach, J. Horwath, M. Knapek, N. Perlot, K. Arai, T. Jono, Y. Koyama, N. Kura, and K. Ohinata, "Report on dlr-jaxa joint experiment: The Kirari optical downlink to Oberpfaffenhofen (KIODO)," Japan Aerospace Exploration Agency (JAXA), Tech. Rep., 2007.

[14] G. Böcherer, "Achievable rates for shaped bit-metric decoding," *arXiv preprint arXiv:1410.8075*, 2014.

[15] G. Caire, G. Taricco, and E. Biglieri, "Bit-interleaved coded modulation," *IEEE Trans. Inf. Theory*, vol. 44, no. 3, pp. 927–946, 1998.

[16] A. Shrestha, D. Giggenbach, and N. Hanik, "Delayed frame repetition for free space optical communication (FSO) channel," in *Photonic Networks; 18. ITG-Symposium*, Leipzig, Germany, Jul. 2017, pp. 1–5.

[17] C. Schieler, A. S. Garg, B. Bilyeu, J. P. Wang, and B. S. Robinson, "Demonstration of reliable high-rate optical communication over an atmospheric link using ARQ," in *Int. Conf. Space Opt. Sys. and Appl. (ICSOS)*, Portland, OR, USA, Oct. 2019, pp. 1–6.

[18] *Optical communications and physical layer coding*, Pink sheets, Consultative Committee for Space Data Systems (CCSDS) Draft Recommended Standard 141.0-P-1.1, Jul. 2020.

[19] D. Divsalar, S. Dolinar, and C. Jones, "Low-rate LDPC codes with simple protograph structure," in *Proc. IEEE Int. Symp. Inf. Theory (ISIT)*, Sep. 2005, pp. 1622–1626.

[20] F. Steiner, G. Böcherer, and G. Liva, "Protograph-based LDPC code design for shaped bit-metric decoding," *IEEE J. Sel. Areas Commun.*, vol. 34, no. 2, pp. 397–407, 2016.

[21] J. Boutros, A. Guillen i Fabregas, and E. Calvanese, "Analysis of coding on non-ergodic block fading channels," in *Allerton Conf. Commun., Contr., Comput.*, Allerton, IL, USA, Oct. 2005.